

Fault-tolerant quantum computation in concatenation of verified cluster states

Keisuke Fujii and Katsuji Yamamoto

Department of Nuclear Engineering, Kyoto University, Kyoto 606-8501, Japan

(Dated: February 6, 2020)

A novel scheme is presented for fault-tolerant quantum computation based on the cluster model. Some relevant logical cluster states are constructed in concatenation by post-selection through verification, without necessity of recovery operation, where a suitable code such as the Steane's 7-qubit code is adopted for transversal operations. This simple concatenated construction of verified cluster states achieves a high noise threshold $\sim 1\%$, and restrains the divergence of resources.

PACS numbers: 03.67.Lx, 03.67.Pp, 03.67.-a

In order to implement reliable computation in physical systems, the problem of noise should be overcome. Then, fault-tolerant quantum computation with error correction has been investigated [1, 2, 3, 4, 5, 6, 7]. In the usual quantum error correction (QEC), error syndromes are detected on encoded qubits, and the errors are corrected according to them. The noise thresholds for fault-tolerant computation are calculated to be about $10^{-6} - 10^{-3}$ depending on the QEC protocols and noise models [6, 7, 8, 9, 10, 11, 12, 13, 14, 15]. A main motivation for QEC comes from the fact that in the circuit model the original qubits should be used throughout computation even if errors occur on them.

On the other hand, more robust computation may be performed in measurement-based quantum computers [16, 17, 18, 19, 20, 21, 22]. Teleportation from old qubits to fresh ones is made by measurements implementing gate operations, and the original qubits are not retained. Then, even recovery operation may not be required. An interesting computation model with error-correcting teleportation is proposed based on encoded Bell pair preparation and Bell measurement, which provides a high noise threshold $\sim 3\%$ [20, 21]. The cluster model or one-way computer [18] should also be considered for fault-tolerant computation. A highly entangled state, called a cluster state, is prepared, and gate operations are implemented by measuring the qubits in the cluster with feedforward for the post-selection of measurement bases. This gate operation in the cluster model may be viewed as the one-bit teleportation [17]. A promising scheme for linear optical quantum computation is proposed, where deterministic gates are implemented by means of the cluster model [23]. Fault-tolerant computation is built up for this optical scheme by using a clustered version of the syndrome extraction for QEC [6]. The noise thresholds are estimated to be about 10^{-3} for photon loss and 10^{-4} for depolarization [24]. The threshold result is also argued by simulating the QEC circuits with clusters [25, 26, 27].

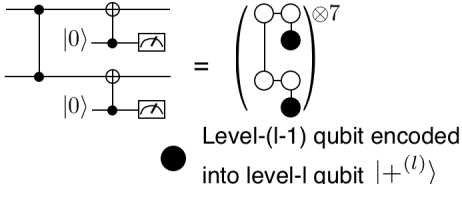
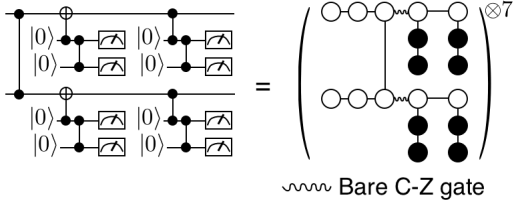
In this Letter, we propose a novel scheme of fault-tolerant quantum computation by making a better use of the unique feature of the cluster model, that is, once clusters are prepared they are just consumed by measurements for computation. Specifically, the fault-tolerant computation is implemented by *concatenated construction and verification of logical cluster states by post-*

selection. A number of relevant logical cluster states are constructed in parallel through verification, and the unsuccessful ones are discarded. This enables the creation of clean clusters by post-selection to achieve a high noise threshold $\sim 1\%$. The high fidelity preparation of ancillary Bell states is adopted for the error-correcting teleportation [20, 21]. It is also considered that improved ancilla preparation increases the noise threshold [28, 29]. In the present scheme, even gate operations, which are represented by cluster states, are verified and post-selected before computation to reduce errors efficiently. (See Refs. [20, 21, 22] for related works.) This is quite distinct from the circuit-based QEC methods, where error corrections should be made after noisy gate operations. Furthermore, the concatenated construction of verified clusters is suitable to restrain the divergence of resources for a large size computation. The concatenation is made readily by adopting a class of stabilizer codes of Calderbank-Shor-Steane (CSS), e.g., the Steane's 7-qubit code [2, 3, 14]. The logical measurements of Pauli operators as well as some relevant Clifford gates, H , S and $C-Z$, are implemented transversally on such a quantum code. It is even the case that the non-Clifford $\pi/8$ gate for universal computation is implemented by preparing a specific qubit and making a transversal measurement.

The construction of the relevant cluster states through verification is made at each logical level as follows.

(i) *Single and double verifications*: A single verification at the logical level- l ($l \geq 1$) is implemented by using transversally 1×7 level- l hexa-clusters in Fig. 1. [The hexa-cluster consisting of 6 level- $(l-1)$ qubits is called as the level- l together with the level- l ancilla qubits (Fig. 4).] Here, each level- $(l-1)$ \bullet qubit is connected through a H rotation to a level- $(l-1)$ \odot qubit in a verified ancilla $|+\rangle^{(l)}$ (Fig. 4) with a *bare* $C-Z$ gate (transversal concatenation of physical $C-Z$ gates without verification). This verification extracts the error syndrome [6, 7, 8] of the two qubits through a $C-Z$ gate (see the circuit diagram in Fig. 1). A double verification is also implemented with 3×7 level- l hexa-clusters in Fig 2, where the wavy lines denote the bare $C-Z$ connections. Here, even the errors in the ancilla \bullet qubits are detected for higher fidelity.

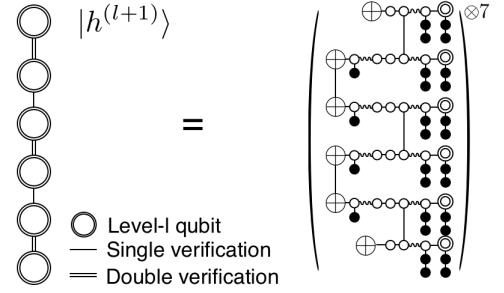
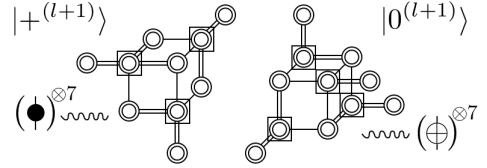
It should be mentioned that particularly for the level-1 verification the circuit diagrams in Figs. 1 and 2 or their minimum cluster equivalents ($C\text{-Not} \rightarrow C\text{-}H\text{Z}H$) may be

FIG. 1: Single verification at the level- l .FIG. 2: Double verification at the level- l .

used to optimize the efficiency. The use of hexa-clusters at the level-1, which are simply the combinations of physical qubits connected with bare C-Z gates, is rather redundant and noisy.

(ii) *Hexa-cluster and ancilla qubits:* The level- $(l+1)$ hexa-cluster $|h^{(l+1)}\rangle$ ($l \geq 1$) is constructed in Fig. 3 by combining transversally the level- l hexa-clusters $|h^{(l)}\rangle$ with bare C-Z connections (wavy lines) to implement 2 single verifications (single lines) and 3 double ones (double lines) at the level- l . (As mentioned above, the level-1 verification may be implemented based on the circuit diagrams, without using the level-1 hexa-clusters.) Here, the level- $(l-1)$ \oplus and \bullet qubits are connected through the H rotation to the level- $(l-1)$ \odot qubits in $|0^{(l)}\rangle$ and $|+^{(l)}\rangle$, respectively, with the bare C-Z gate. The qubits \oplus , \circ , \bullet are measured in Fig. 3 to construct the $|h^{(l+1)}\rangle$ via one-way computation. If all the level- l measurements, which consist of the transversal measurements of the level- $(l-1)$ \bullet qubits, provide the correct syndrome, the 6 level- l \odot qubits survive passing the verification to form the $|h^{(l+1)}\rangle$. (Otherwise, the unsuccessful case is discarded.) The single and double verifications are suitably combined in such ways that each qubit has at most one bare C-Z connection to keep high fidelity, and that the \odot qubits to survive are doubly verified.

The level-1 $|0^{(1)}\rangle$ and $|+^{(1)}\rangle$ are encoded with physical qubits and gate operations, and they are verified by measuring the stabilizer and extracting the error syndrome to remove sufficiently the depolarization errors [6, 7, 8]. (The meaningless level-0 hexa-clusters cannot be used for this verification.) Then, the level- $(l+1)$ $|+^{(l+1)}\rangle$ and $|0^{(l+1)}\rangle$ ($l \geq 1$) are constructed through the verification in Fig 4, similarly to the hexa-cluster $|h^{(l+1)}\rangle$. They are the code blocks consisting of the 7 doubly-verified level- l \odot qubits, and the boxed \odot qubits are measured for H rotations.

FIG. 3: Hexa-cluster at the level- $(l+1)$.FIG. 4: Ancilla qubits at the level- $(l+1)$.

(iii) *Universal computation:* The verified clusters $|h^{(l+1)}\rangle$, $|+^{(l+1)}\rangle$, $|0^{(l+1)}\rangle$ are constructed up to the highest logical level to achieve the fidelity required for a given computation size. Then, the computation is implemented by combining suitably these highest level clusters with bare C-Z gates and measuring the qubits.

The non-Clifford $|\pi/8\rangle = \cos(\pi/8)|0\rangle + \sin(\pi/8)|1\rangle$ is also prepared for universal computation, as seen below. The operation $HZ(\theta) = He^{-i\theta Z/2}$ is implemented by the measurement in the basis $Z(\pm\theta)\{|+\rangle, |-\rangle\}$ to be post-selected by the outcome of preceding measurements [18]. The non-Clifford $\pi/8$ gate $Z(\pi/4)$, however, does not operate transversally even on the 7-qubit code. We here exchange the $Z(\pm\pi/4)$ rotation and the C-Z gates between the original $|+\rangle$ and the measurement. Then, the operation $HZ(-\pi/4)$ for the $\pi/8$ gate is equivalently implemented by the preparation of $Z(-\pi/4)|+\rangle$ and the measurement with post-selection of I or $S = Z(\pi/2)$. In this way, we can implement the H , S , $\pi/8$ and C-Z gates as a universal set by transversal measurements.

The preparation of $Z(-\pi/4)|+\rangle$ is based on the relation $Z(-\pi/4)|+\rangle = e^{i\phi}HS|\pi/8\rangle$ with certain phase ϕ . The level-1 $|\pi/8^{(1)}\rangle$ is first encoded with physical qubits as given in Ref. [12]. Then, the higher level $|\pi/8^{(l+1)}\rangle$ is constructed with the lower level $|\pi/8^{(l)}\rangle$ in a similar diagram to Fig. 4. It should be noted here that the prepared level-1 $|\pi/8^{(1)}\rangle$ may contain a small mixture of $|5\pi/8^{(1)}\rangle$ on the code space. This logical failure cannot be detected in encoding the level-2 $|\pi/8^{(2)}\rangle$, because the orthogonal $|5\pi/8^{(2)}\rangle$ has the correct syndrome. Similarly, the small mixture of $|5\pi/8^{(l)}\rangle$ is not reduced by the concatenation, though the constructed $|\pi/8^{(l)}\rangle$ is kept on the code space

by the verification, retaining the logical fidelity as the $|\pi/8^{(1)}\rangle$. This slightly noisy $|\pi/8^{(l)}\rangle$ is, however, sufficient for universal computation at the highest level. We can obtain the high fidelity $|\pi/8^{(l)}\rangle$ by using Clifford operations according to the magic state distillation [30].

The errors in computation should be calculated properly in the present scheme to estimate the noise threshold, where the concatenated construction of verified clusters is provided fault-tolerantly. Specifically, we need to consider the errors on the cluster states and Pauli frames.

(i) *Homogeneous errors in qubits:* At the beginning of concatenation, the level-1 qubits to form the level-2 cluster states are doubly verified with transversal gates and measurements. Then, it is reasonably expected that the level-0 qubits encoded in these level-1 qubits contain independently and identically distributed (homogeneous) depolarization errors in the leading order [29]. The homogeneous error probabilities ϵ_A ($A = X, Y, Z$) of these level-0 qubits are determined in terms of the error probabilities p_{AB} of the physical gates which are used for the level-1 double verification. At the higher levels, hexa-clusters, bare C-Z gates and measurements are used for the verified construction in the cluster diagrams (Fig. 3). Any operations are, however, not made directly on the level- l \odot qubits to form the level- $(l+1)$ clusters. Then, these level- l qubits inherit transversally the homogeneous errors ϵ_A of the level-0 qubits. In the case of level- l qubits which have one bare C-Z connection (wavy line) to implement the upper-level construction, extra errors are added transversally to the component level-0 qubits through the physical C-Z gate as (summed over $B = I, X, Y, Z$)

$$\begin{aligned}\epsilon'_X &= \epsilon_X + p_{XB}, \epsilon'_Y = \epsilon_Y + p_{YB}, \\ \epsilon'_Z &= \epsilon_Z + \epsilon_X + \epsilon_Y + p_{ZB},\end{aligned}\quad (1)$$

where $\epsilon_X = p_{XI}$, $\epsilon_Y = p_{YI}$, $\epsilon_Z = 2p_{ZI}$ from the circuit diagram in Fig. 2 with physical C-Z and C-Not gates.

(ii) *Errors in measurements and threshold:* By the measurements of qubits in implementing the verified cluster construction (Fig. 3), the Pauli frames of the neighboring qubits are updated. The level- l \odot qubits are, however, always checked by the double verification at the final step (each \odot has at least one double-line connection in Figs. 3 and 4) so that the Pauli frame errors are not propagated to them. That is, if the concatenated construction is made successfully from the level-1 to the level- $(l+1)$, it is ensured that the Pauli frame errors are absent in the leading order on the level- l qubits to form the level- $(l+1)$ clusters. Hence, the error probabilities $p_{n,b}^{(l)}$ for the measurements of these qubits (normal and bare-connected) are simply determined on the 7-qubit code with distance 3 by the recurrence relation as

$$p_{n,b}^{(l)} \simeq 7C_2(p_{n,b}^{(l-1)})^2 \simeq (7C_2 p_{n,b}^{(0)})^{2^l} / 7C_2. \quad (2)$$

These measurement errors are propagated as the Pauli frame errors to the neighboring qubits, and they are removed by post-selection at the final step of verification.

The level-0 qubits contained in the verified clusters have the homogeneous errors ϵ_A and ϵ'_A . They are measured with the error probabilities $p_n^{(0)} = \epsilon_Z + \epsilon_Y + p_M$ and $p_b^{(0)} = \epsilon'_Z + \epsilon'_Y + p_M$, where p_M is the error probability of physical measurement. Then, the noise threshold is determined in Eq. (2) ($p_b^{(0)} > p_n^{(0)}$ with $\epsilon'_A > \epsilon_A$) as

$$p_b^{(0)} = \epsilon'_Z + \epsilon'_Y + p_M \equiv Dp_e < 1/7C_2 \rightarrow p_{\text{th}}, \quad (3)$$

where p_e represents the mean error probability of physical operations ($D \sim 1$). The noise threshold is estimated as

$$p_{\text{th}} = (7C_2 D)^{-1} = 0.042 (D = 17/15) \quad (4)$$

typically for $p_{AB} = (1/15)p_e$ in Eq. (1) and $p_M = (4/15)p_e$ [21]. We have made a numerical simulation to confirm the above estimates concerning the errors on the qubits and Pauli frames in the concatenation. It is checked that the Pauli frame errors on the successful \odot qubits are absent in the leading order, as considered in Eq. (2).

We next calculate the physical resources (qubits and gates) in the recurrence relations by counting the numbers of hexa-clusters, ancilla qubits, and bare C-Z gates in Figs. 1 (S), 2 (D), 3 (h) and 4 (0 and +):

$$R_S^{(l)} = 7R_h^{(l)} + 2(R_+^{(l)} + R_b^{(l)})(l \geq 2), \quad (5)$$

$$R_D^{(l)} = 3 \times 7R_h^{(l)} + 8(R_+^{(l)} + R_b^{(l)}) + 2R_b^{(l)}(l \geq 2), \quad (6)$$

$$R_\alpha^{(l+1)} = \sum_{O=S,D,0,b} n_\alpha^O R_O^{(l)} / p_\alpha^{(l+1)}(l \geq 1), \quad (7)$$

where $R_b^{(l)} = 7^l$ for a bare C-Z gate, $(n_\alpha^S, n_\alpha^D, n_\alpha^0, n_\alpha^b) = (2, 3, 6, 4)_h, (6, 7, 11, 15)_0, (5, 6, 10, 14)_+$ for $|\alpha\rangle = |h\rangle, |0\rangle, |+\rangle$, respectively ($n_\alpha^0 \rightarrow n_\alpha^+$ and $n_\alpha^b = 0$ at the level-1), and the success probabilities $p_\alpha^{(l+1)}$ for the cluster verification are taken into account. The physical resources at the level-1 are given by $R_0^{(1)} = 69(95)/p_0^{(1)}$, $R_+^{(1)} = 72(109)/p_+^{(1)}$, $R_S^{(1)} = 3(11) \times 7 + 2R_0^{(1)}$, $R_D^{(1)} = 9(17) \times 7 + 8R_0^{(1)}$ with physical C-Not and C-Z gates (or C-Not \rightarrow C-HZH as 1 gate \rightarrow 3 gates and 2 qubits).

The success probabilities $p_\alpha^{(l)}$ are evaluated by the numerical simulation, which approach unity at the level-3 or higher as the logical measurement errors $p_{n,b}^{(l)}$ are reduced rapidly below the threshold. The resources usage are estimated in the above recurrence relations with these $p_\alpha^{(l)}$, depending on the computation size N with the highest level $l \sim \log_2(\log_{10} N)$ to achieve the accuracy $0.1/N$. The results ($R_0^{(l)}$, which is larger than $R_{h,+}^{(l)}$) are shown in Fig. 5 for the present scheme of verified logical clusters (LC) with $p_e = 10^{-2}$ (physical C-Not and C-Z for the level-1 construction) and 10^{-3} (C-Not \rightarrow C-HZH for the physical cluster model), which are compared to the circuit-based Steane's QEC scheme with $p_e = 10^{-3}$ [9]. Each step in these graphs means the up of logical level by one. The present scheme really consumes much less resources than the Steane's QEC scheme for $p_e \leq 10^{-3}$.

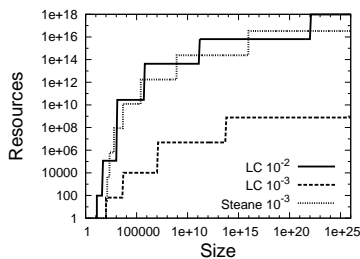


FIG. 5: Resources usage for the present scheme of verified logical clusters (LC) with $p_e = 10^{-2}$ (physical C-Not and C-Z) and 10^{-3} (physical cluster model), which are compared to the Steane's QEC scheme with $p_e = 10^{-3}$.

We also find that compared to the C_4/C_6 scheme with post-selection (with error-correction) [20, 21], the present scheme with much simpler concatenation provides a comparable threshold, requiring much less (comparable) resources. Furthermore, the present scheme has a lot of room for improvement. The Fibonacci scheme based on the 4-qubit error-detecting code may be applied to improve the performance, especially the resources. The optimal decoding (adaptive concatenation) scheme [31] is available without any change. This will boost the noise threshold up to about 9%, and save the resources sufficiently below the threshold.

The memory errors may be significant in this post-selection scheme without recovery operation. The qubits to form the clusters are not touched directly (but via the one-bit teleportation) in the verified construction

after the level-1 double verification. Then, the memory errors accumulate until they are measured in the upper-level construction. The memory errors are added as $p_{n,b}^{(0)} + \ln \tau_M p_e$, where $\tau_M p_e$ denotes the probability of memory error with the effective waiting time τ_M for one measurement, and n is the number of waiting time steps at each concatenation level (e.g., $n = 12$ for the hexa-cluster). The noise threshold is hence determined as $p_{th} \sim [{}_7C_2 \{1 + \log_2(\log_{10} N) n \tau_M\}]^{-1}$, depending on the computation size N with the highest level $l \sim \log_2(\log_{10} N)$. For example, $p_{th} \sim 1\%$ for $N \sim 10^{20}$ and $\tau_M = 0.1$ ($n \sim 10$), which will be tolerable for practical computations. In order to overcome essentially the memory error accumulation, the hexa-cluster as a two-colorable graph state may be refreshed at each concatenation level by using a purification protocol [32].

In summary, we have presented a novel scheme for fault-tolerant quantum computation based on the cluster model. Some relevant logical cluster states are constructed in concatenation by post-selection through verification, without necessity of recovery operation, where a suitable code such as the Steane's 7-qubit code is adopted for transversal operations. This simple concatenated construction of cluster states achieves a high noise threshold $\sim 1\%$, and restrains the divergence of resources. The present scheme consumes much less resources than the usual circuit-based QEC schemes for the physical error probability $\leq 10^{-3}$.

This work was supported by International Communications Foundation (ICF).

-
- [1] P. W. Shor, Phys. Rev. A **52**, R2493 (1995).
 - [2] A. R. Calderbank and P. W. Shor, Phys. Rev. A **54**, 1098 (1996).
 - [3] A. M. Steane, Phys. Rev. Lett. **77**, 793 (1996).
 - [4] P. W. Shor, *Proceedings of the 37th Annual Symposium on Foundations of Computer Science* (IEEE Computer Society Press, Los Alamitos, CA, 1996), p. 56.
 - [5] D. P. DiVincenzo and P. W. Shor, Phys. Rev. Lett. **77**, 3260 (1996).
 - [6] A. M. Steane, Phys. Rev. Lett. **78**, 2252 (1997).
 - [7] A. M. Steane, Fortschr. Phys. **46**, 443 (1998).
 - [8] A. M. Steane, Nature **399**, 124 (1999).
 - [9] A. M. Steane, Phys. Rev. A **68**, 042322 (2003).
 - [10] A. Yu. Kitaev, Russ. Math. Surv. **52**, 1191 (1997).
 - [11] J. Preskill, Proc. R. Soc. London A **454**, 385 (1998).
 - [12] E. Knill, R. Laflamme, and W. H. Zurek, Proc. R. Soc. London A **454**, 365 (1998); Science **279**, 342 (1998).
 - [13] D. Gottesman, Ph.D. thesis, California Institute of Technology (1997).
 - [14] D. Gottesman, Phys. Rev. A **57**, 127 (1998).
 - [15] D. Aharonov and M. Ben-Or, *Proceedings of the 29th Annual ACM Symposium on the Theory of Computation* (ACM Press, New York, 1998), p. 176.
 - [16] D. Gottesman and I. L. Chuang, Nature **402**, 390 (1999).
 - [17] X. Zhou, D. W. Leung, and I. L. Chuang, Phys. Rev. A **62**, 052316 (2000).
 - [18] R. Raussendorf and H. J. Briegel, Phys. Rev. Lett. **86**, 5188 (2001); R. Raussendorf, D. E. Browne, and H. J. Briegel, Phys. Rev. A **68**, 022312 (2003).
 - [19] M. A. Nielsen, Phys. Lett. A **308**, 96 (2003).
 - [20] E. Knill, Phys. Rev. A **71**, 042322 (2005).
 - [21] E. Knill, Nature **434**, 39 (2005).
 - [22] M. Silva, V. Danos, E. Kashefi, and H. Ollivier, New J. Phys. **9**, 192 (2007).
 - [23] M. A. Nielsen, Phys. Rev. Lett. **93**, 040503 (2004).
 - [24] C. M. Dawson, H. L. Haselgrove, and M. A. Nielsen, Phys. Rev. Lett. **96**, 020501 (2006); Phys. Rev. A **73**, 052306 (2006).
 - [25] R. Raussendorf, Ph.D. thesis, Ludwig-Maximilians Universität München (2003).
 - [26] M. A. Nielsen and C. M. Dawson, Phys. Rev. A **71**, 042323 (2005).
 - [27] P. Aliferis and D. W. Leung, Phys. Rev. A **73**, 032308 (2006).
 - [28] B. W. Reichardt, quant-ph/0406025 (2004).
 - [29] B. Eastin, Phys. Rev. A **75**, 022301 (2007).
 - [30] S. Bravyi and A. Kitaev, Phys. Rev. A **71**, 022316 (2005).
 - [31] D. Poulin, Phys. Rev. A **74**, 052333 (2006); J. Fern, Phys. Rev. A **77**, 010301(R) (2008).
 - [32] W. Dür, H. Aschauer, and H. J. Briegel, Phys. Rev. Lett. **91**, 107903 (2003); H. Aschauer, W. Dür, and H. J. Briegel, Phys. Rev. A **71**, 012319 (2005).